Meshless Radial Basis Functions Method for Solving Hallen's Integral Equation

Sheng-Jian Lai, Bing-Zhong Wang, and Yong Duan

Abstract—This paper introduced a meshless method based on radial basis function (RBF) interpolation to solve Hallen's integral equation (HIE) of the thin wire. The unknown current $I_z(z)$ is interpolated by RBF at the center nodes and point matching method is applied to HIE at the collocation nodes. To validate the present method, the input impedance and induced current of dipole antenna are computed with the r^5-RBF and Wu's RBF, respectively. The results show that the present method is a steady numerical approach for solving HIE.

Index Terms—Hallen's integral equation, meshless method, point matching method, radial basis functions.

I. INTRODUCTION

In the past several decades, various numerical techniques have been used to solve Hallen's integral equation (HIE) and evaluate electromagnetic field, induced current distribution, and input impedance of thin linear antenna. Mei firstly proposed classical moment method (MOM) to solve HIE [1]. Now, various advanced numerical approaches were applied to HIE, such as high accurate computation[2], hybrid procedure[4], Galerkin's methods [5], high-order numerical solution [6], entire-domain basis functions in Galerkin's methods [7], and some combined algorithm with MOM[3].

The techniques mentioned above are grid-based or mesh-based ones. In recent years, meshfree or meshless methods (MLMs) based on a set of nodes scattering within the problem domain have gained much attention in the engineering communities [8] and significantly developed in the electromagnetic engineering area [9]-[11]. Nicomedes proposed the improve Moving Least Square to solve the combined field integral equation [12]. Galerkin-Bubnov Integral Equation Method [13] was used to solve time-domain HIE. In this paper, we introduce a meshless method based on radial basis function interpolation (MLM-RBF) to solve HIE. RBF interpolation is a powerful technique that was first proposed by Kansa in 1990 to solve partial difference equations (PDEs) [14]. MLM-RBF is a numerical method by which unknown functions of PDEs or integral equations are interpolated at the scattered nodes and point matching method is applied to the equations at the collocation nodes.

Section II describes the MLM-RBF formulation of HIE. It also presents the process of impedance matrix calculation. In Section III, the numerical results using two different RBFs are discussed in detail. Conclusion is given in Section IV.

II. FORMULATION

Figure 1 shows a perfectly conducting long and $\hat{z}$ -oriented thin wire of L in length whose radius R_0 is much less than L and wavelength λ. The HIE of the thin and straight wire can be expressed as [15]

$$E_z^i(z) = \frac{j}{\omega\varepsilon}\left[\frac{\partial}{\partial z^2} + k^2\right]\int_{-L/2}^{L/2} I_z(z')\frac{e^{-jkR}}{4\pi R}dz' \quad (1)$$

where $R = \sqrt{(z-z')^2 + a^2}$ and k represents propagation constant. Through a series of processing steps [15], the above equation can be simplified as

$$\int_{-L/2}^{L/2} I_z(z')\frac{e^{-jkR}}{4\pi R}dz' = D_1 e^{jkz} + D_2 e^{-jkz} + \frac{1}{2\eta}\int_{-L/2}^{L/2} e^{-jk|z-z'|}E_z^i(z')dz' \quad (2)$$

where η is wave impedance, D_1 and D_2 are unknown constants.

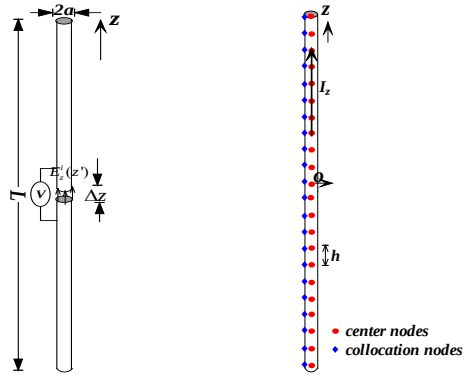

(a) (b)

Fig. 1. Model of thin wire (a) and node distribution (b).

The unknown function I_z in (2) can be interpolated approximately by a series of RBF:

Submitted On: March 10, 2011
Accepted On: Jan 26, 2012

$$I_z(z) \approx \sum_{I=1}^{N} \phi_I(z) a_I = \sum_{I=1}^{N} \phi(|z - z_I|) a_I, \quad z \in [-L/2, L/2] \quad (3)$$

where $\phi_I(\boldsymbol{r})$ is the radial basis function centered at a set of independent points $\boldsymbol{r}_1, \cdots, \boldsymbol{r}_I, \cdots, \boldsymbol{r}_N \in \Omega$ (also called center nodes, see Fig.1 (b)). a_I are unknown coefficients to be computed.

Substituting (3) into (2), we get

$$\sum_{I=1}^{N} a_I \int_{L_I} \phi_I(z') \frac{e^{-jkR}}{4\pi R} dz' = D_1 e^{jkz} + D_2 e^{-jkz} + \frac{1}{2\eta} \int_{-L/2}^{L/2} e^{-jk|z-z'|} E_z^i(z') dz' \quad (4)$$

where L_I is the integral domain at the center node z_I and $\phi_I(z') = \phi(|z' - z_I|)$. Then, point-matching method (PMM) is applied to the above equation at a set of collocation nodes $z_1, \cdots, z_J, \cdots, z_M$ ($M \geq N$) (see Fig.1 (b)) which distribute on the wire surface. Thus, we get

$$\sum_{I=1}^{N} a_I \int_{L_I} \phi(|z' - z_I|) \frac{e^{-jkR_J}}{4\pi R_J} dz' = D_1 e^{jkz_J} + D_2 e^{-jkz_J} + \frac{1}{2\eta} \int_{-L/2}^{L/2} e^{-jk|z_J - z'|} E_z^i(z') dz' \quad (5)$$

where $R_J = \sqrt{(z_J - z')^2 + a^2}$. The resulting matrix of the above equation is of the form

$$\mathbf{Z}\mathbf{a} = [\mathbf{s}_1, \mathbf{s}_2][D_1, D_2]^T + \mathbf{b}, \quad (6)$$

where the elements of impedance matrix $\mathbf{Z}$ are

$$z_{IJ} = \int_{L_I} \phi(|z' - z_I|) \frac{e^{-jkR_J}}{4\pi R_J} dz', \quad (7)$$

and the vector elements of right-hand side of (6)

$$s_{1J} = e^{jkz_J}, s_{2J} = e^{-jkz_J}$$
$$b_J = \frac{1}{2\eta} \int_{-L/2}^{L/2} e^{-jk|z_J - z'|} E_z^i(z') dz' \quad (8)$$

A. Calculation of unknown constant D_1 and D_2

To obtain the unknown vector **a** in (6), the constant D_1 and D_2 should be determined first. This can be done by using the current boundary condition at the ends of the wire, i.e., $\boldsymbol{I}_z(-L/2)=\boldsymbol{I}_z(L/2)=0$. From(6), we have

$$\mathbf{a} = \mathbf{Z}^{-1}[\mathbf{s}_1, \mathbf{s}_2][D_1, D_2]^T + \mathbf{Z}^{-1}\mathbf{b} \quad (9)$$

Defining $[\mathbf{U}] = [\mathbf{u}_1^T, \mathbf{u}_2^T]$, where $\mathbf{u}_1^T$ =[1,0,...,0] and $\mathbf{u}_2^T$ =[0,...,0,1] and multiplying both sides of (9) by $[\mathbf{U}]^T$, we get

$$[\mathbf{U}]^T \mathbf{a} = [\mathbf{U}]^T \mathbf{Z}^{-1}[\mathbf{s}_1, \mathbf{s}_2][D_1, D_2]^T + [\mathbf{U}]^T \mathbf{Z}^{-1}\mathbf{b} = 0, \quad (10)$$

Solving (10), we get

$$[D_1, D_2]^T = -\left[[\mathbf{U}]^T \mathbf{Z}^{-1}[\mathbf{s}_1, \mathbf{s}_2]\right]^{-1} [\mathbf{U}]^T \mathbf{Z}^{-1}\mathbf{b} \quad (11)$$

B. Calculation of matrix element

When the collocation node z_J does not locate in the range of the supported domain centered at z_I, the matrix elements of (7) can be computed via an Q-point numerical quadrature [15]:

$$z_{IJ} = \sum_{q=1}^{Q} w_q \phi_I(|z_{Iq} - z_I|) \frac{e^{-jkR_{J\_Iq}}}{4\pi R_{J\_Iq}}, \quad I \neq J \quad (12)$$

where $R_{J\_Iq} = \sqrt{(z_J - z_{J\_Iq})^2 + a^2}$.

When z_J locates in the range of the supported domain centered at z_I, as shown in Fig. 2, there exists the quasi-singular integral in (7). To improve the integral accuracy, a very small domain Δ_z centered at z_J is extracted from L_I of (7). Thus, there exist three integral domains in L_I: $[z_I - d_{mI}, z_J - \Delta_z/2]$, $[z_J - \Delta_z/2, z_J + \Delta_z/2]$, and $[z_J + \Delta_z/2, z_I + d_{mI}]$ (see Fig.2), where d_{mI} is the radius of supported domain of RBF centered at z_I. In Δ_z, the integral item $\phi(|z' - z_I|)$ in (7) is treated as a constant value $\phi(|z_J - z_I|)$ and the Green's function item is expanded by the small-argument approximation [15]. Thus, (7) in the integral domain Δ_z can be rewritten as:

$$\int_{-\Delta_z/2}^{\Delta_z/2} \phi(|z' - z_I|) \frac{1 - jkR_J}{4\pi R_J} dz' = \phi(|z_J - z_I|) \left[\frac{1}{4\pi} \ln \left(\frac{\sqrt{1 + 4a^2/\Delta_z^2} + 1}{\sqrt{1 + 4a^2/\Delta_z^2} - 1} \right) - \frac{jk\Delta_z}{4\pi} \right], I = J \quad (13)$$

In other two domains, (7) is also computed by the Q-point numerical quadrature (12).

Each element in (7) needs to be calculated with the Q-point numerical quadrature, not a simple expression in MOM [15]. Thus, the amount of calculation of MLM-RBF is more than that of MOM in solving HIE.

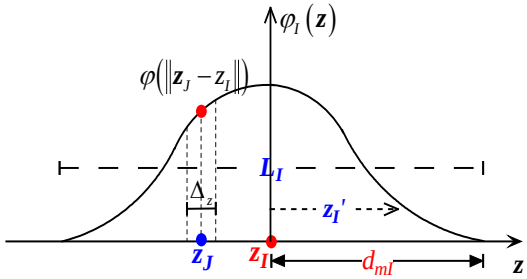

Fig. 2. Collocation node z_J located in the range of the supported domain centered at z_I

From (6), the unknown coefficient vector **a** can be solved. Then substituting **a** into(3), we can get the current distribution of the thin wire.

III. Numerical Results

In order to validate the present method, the input impedance and induced current distribution of a thin wire are calculated by MLM-RBF. Here, a delta-gap

source $E_z^i(z') = \delta(z')$ at the center of the wire is adopted, as shown in Fig. 1(a). The length and radius of the wire are set as $L=\lambda/2$ and $a=10^{-3}\lambda$, respectively. Uniform node distribution is adopted on the wire axis and the distance between nodes is h. To analyze the accuracy of the present numerical algorithm, the results of MLM-RBF are compared with those of mesh-based MOM on the condition that the node distribution (grid distribution) is the same. In this work, two different kinds of MOM are taken as referenced methods, which are PMM with pulse basis function and Galerkin's method with triangle basis function. The former is directly used to solve HIE and this process is called Hallen/Pulse approach. The later is used to solve electric field integral equation (EFIE) of arbitrarily shaped thin wired (ATW) model [15] and this process is called ATW/Triangle approach.

There are many different types of RBFs. Here, two typical RBFs are chosen. One is the quintic RBF:

$$\phi_I(\boldsymbol{r}) = r^5 \tag{14}$$

which is a globally supported RBF without shape parameter. Another is the compactly supported RBF given by Wu [16]:

$$\phi_I(\boldsymbol{r}) = (1-r)_+^6 \left(6+36r+82r^2+72r^3+30r^4+5r^5\right) \tag{15}$$

where $r = \|\boldsymbol{r}-\boldsymbol{r}_I\|/d_{mI}$, and

$$(1-r)_+ = \begin{cases} 1-r & 0 \le r \le 1 \\ 0 & other \end{cases} \tag{16}$$

First, we compare the rates of convergence of the input impedance versus the node number by MLM-RBF with those by referenced methods. Figure 3 (a) shows the results of $\boldsymbol{r}^5$ RBF-based MLM (MLM-r^5-RBF). We can see that, like ATW/Triangle approach, the input impedance of MLM-RBF converges fast to a stable value when the node number is only 12 (i.e. 24 nodes per wavelength). In sharp contrast to r^5-RBF case, the input impedance of the Hallen/Pulse approach converges slowly: more than 200 segments are needed to obtain a good convergence. However, the results of MLM-r^5-RBF could be inaccurate when node number exceeds 90. This is because the condition number of impedance matrix constructed by r^5 RBF is too large (more than 10^{14}) when node number exceeds 90. The r^5 RBF is a power function, its value at the center point is zero. Its conforming impedance matrix is not strictly diagonally dominant matrices that condition number is very large.

In Wu's RBF case (d_{mI}=2.4*h), it can be seen that the input impedance converges more slowly than in r^5 RBF case, but still faster than Hallen/Pulse approach, as shown in Fig. 3 (b). The input resistance computed by Wu's RBF-based MLM (MLM-Wu-RBF) is in good agreement with that by ATW/Triangle approach when node number exceeds 50. For the input reactance of MLM-Wu-RBF, 100 nodes are needed to obtain good convergence results. However, 300 segments are needed for Hallen/Pulse approach. Due to the compactly supported property of Wu's RBF, the generated impedance matrix is strip and sparse. The condition number of the impedance matrix is only 58 when node number reaches 250, which is far less than that of the impedance matrix of r^5 RBF case.

In Wu's RBF case, besides the node number N, there is another parameter d_{mI} to influence the calculation accuracy. Figure 4 shows the input impedance versus d_{mI} of Wu's RBF. From the figure, we can see that the input impedance increases quickly to the peak-value and then decreases slowly as d_{mI} increases. In addition, there exists a range of steady d_{mI} within which the relative errors of peak-value are small. For example, when N=101, the relative error of the peak-value of input resistance is under 1.6% when d_{mI} ranges from 1.8*h to 6*h. From the figure, we can also see that the range of steady d_{mI} widens as the node number increases. General, the d_{mI} parameter of Wu's RBF in HIE is set the 2*h to 5*h that the calculation accuracy is good.

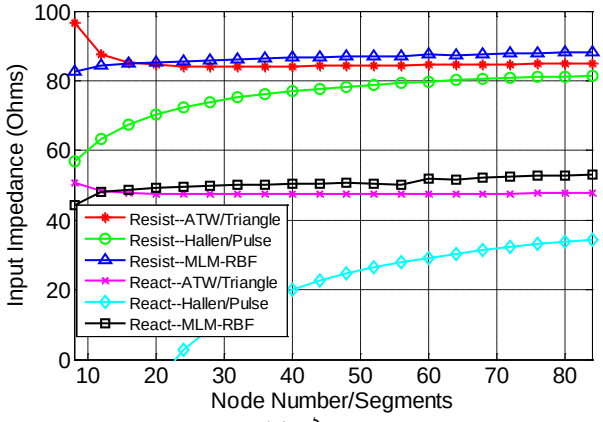

(a) r^5-RBF

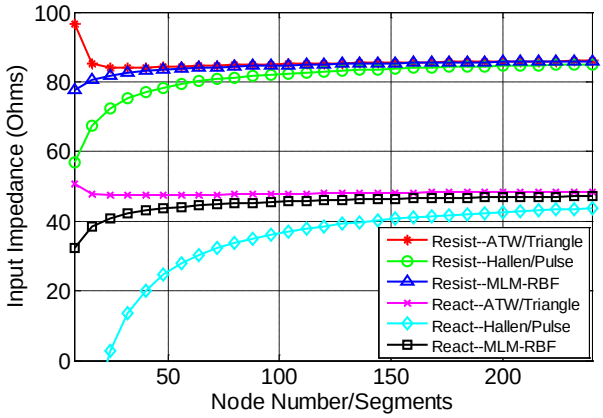

(b) Wu's RBF (d_{mI}=2.4*h)

Fig. 3. Input impedance of a $\lambda/2$ dipole for (a) r^5 RBF and (b) Wu's RBF.

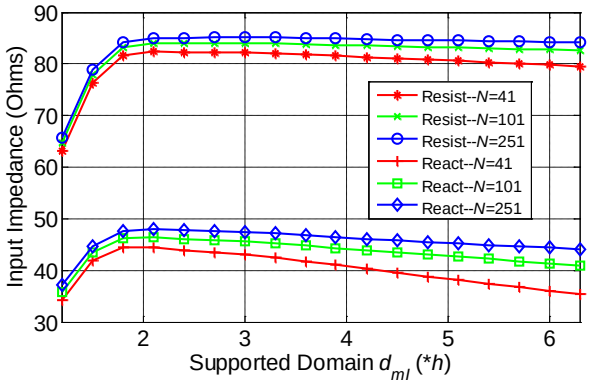

Fig. 4. Input impedance versus supported domain d_{mI} of Wu's RBF.

Then, we compare the induced current distributions between MLM-RBF and reference methods. Figure 5 shows the induced current in r^5 RBF case and induced current versus the d_{mI} in Wu's RBF case when N=41. In r^5 RBF case, the maximum error relative to ATW/ Triangle approach at the center node is 4%. In Wu's RBF case, the maximum error at the center node is 8% when d_{mI} ranges from 1.8*h to 6*h. When d_{mI}= 2.7*h, 4.2*h, and 5.7*h, the current curves are close to those of ATW/Triangle approach. However, when d_{mI} is not within the steady range (from 1.8*h to 6*h), there exist great errors. For example, when d_{mI}= 1.2*h, the maximum error is 36% at the center node.

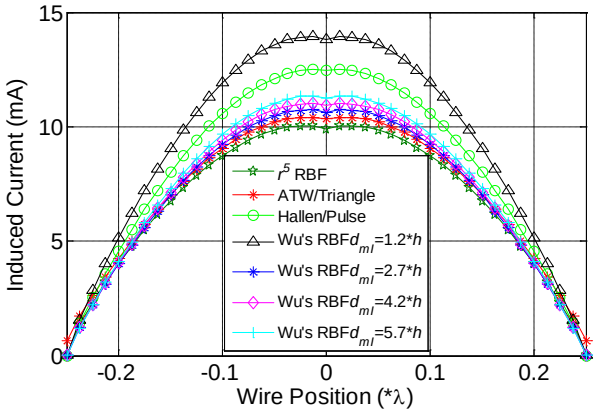

Fig. 5. Induced current distribution on a $\lambda/2$ dipole (node number is 41).

Finally, we consider the generalization of the present method. Taking Wu's RBF for example, we suppose that the d_{mI} is set 2.4*h and a node number per wavelength is at approximately 15, and then the input impedance versus the dipole length ranging from 0.2λ to 3.5λ is computed; the results are shown in Fig. 6. The results of MLM-Wu-RBF are in good agreement with those of ATW/Triangle approach almost at every data point, which seems to show that MLM-Wu-RBF is a feasible and stable algorithm to solving HIE when d_{mI} is in the steady range.

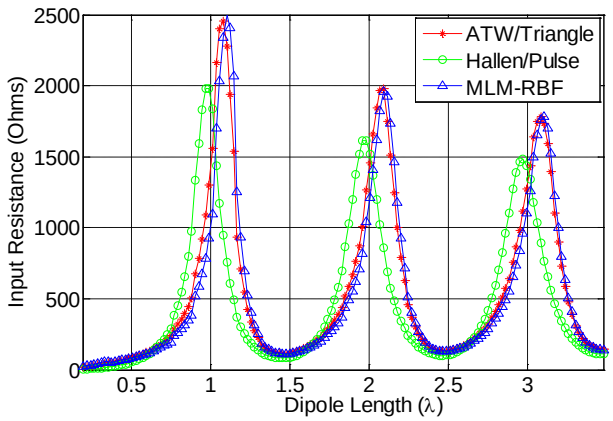

(a) Input Resistance

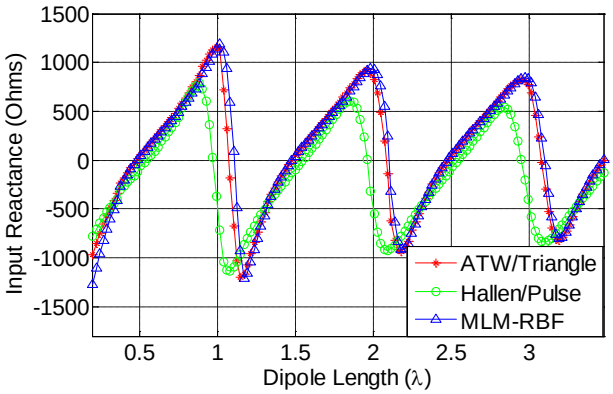

(b) Input Reactance

Fig. 6. Input impedance versus dipole length in Wu's RBF case.

IV. CONCLUSION

In this letter, MLM-RBF is applied to solve HIE of thin wire. The results show that the convergent rates of MLM-RBF are faster than those of MOM. In addition, there exists a steady range of d_{mI} for Wu's RBF within which the results reach certain accuracy. And the steady range of parameter d_{mI} widens as the node number increases. The induced current distributions of r^5 RBF and Wu's RBF within the steady-range parameter d_{mI} are in agreement with the referenced methods. For the r^5 RBF case, the condition number of impedance matrix is too large that some problems cannot be solved. For the Wu's RBF case, when the sample nodes and d_{mI} are set as certain values, the impedances varying with the length of wire are also in agreement with the referenced results, which seems that MLM-RBF can be a general algorithm to computing HIE. But the calculation burden of filling its matrix is somewhat heavier than that of MOM.

REFERENCES

[1] K. K. Mei, "On the Integral Equations of Thin Wire Antennas," *IEEE Trans. Antennas Propag.*, vol. 13, no. 3, pp. 374-378, May 1965.

[2] K. F. A. Hussein, "Accurate Computational Algorithm for Calculation of Input Impedance of Antennas of Arbitrarily Shaped Conducting Surfaces," *Applied*

Computational Electromagnetic Society (ACES) Journal, vol. 22, no. 3, pp. 350–362, November 2007.

[3] R. A. Abd-Alhameed, P. S. Excell, M. A. Mangoud, "Broadband Antenna Response Using Hybrid Technique Combining Frequency Domain MoM and FDTD," *Applied Computational Electromagnetic Society (ACES) Journal,* vol. 20, no. 1, pp. 70–77, Match 2005.

[4] G. Miano, L. Verolino, and V. G. Vaccaro, "A Hybrid Procedure to Solve Hallen's Problem," *IEEE Trans. Electromagn. Compat.,* vol. 38, no. 3, pp. 409-412, Aug. 1996.

[5] G. Fikioris and T. T. Wu, "On the Application of Numerical Methods to Hallen's Equation," *IEEE Trans. Antennas Propag.,* vol. 49, no. 3, pp. 383-392, Mar. 2001.

[6] A. F. Peterson and M. M. Bibby, "High-Order Numerical Solutions of the MFIE for the Linear Dipole," *IEEE Trans. Antennas Propag.,* vol. 52, no. 10, pp. 2684-2691, Oct. 2004.

[7] G. Fikioris and A. Michalopoulou, "On the Use of Entire-Domain Basis Functions in Galerkin Methods Applied to Certain Integral Equations for Wire Antennas with the Approximate Kernel," *IEEE Trans. Electromagn. Compat.,* vol. 51, no. 2, pp. 409-412, May 2009.

[8] G. E. Fasshauer, *Meshfree Approximation Methods with MATLAB*, Singapore: World Scientific Publishing, Chapter 1, 2007.

[9] R. K. Gordon and W. Elliott Hutchcraft, "The Use of Multiquadric Radial Basis Functions in Open Region Problems," *Applied Computational Electromagnetic Society (ACES) Journal,* vol. 21, no. 2, pp. 127–134, July 2006.

[10] S. J. Lai, B. Z. Wang, and Y. Duan, "Meshless Radial Basis Function Method for Transient Electromagnetic Computations," *IEEE Trans. Magn.*, vol. 44, no. 10, pp. 2288–2295, 2008.

[11] X. F. Liu, B. Z. Wang, and S. J. Lai, "Element-Free Galerkin Method for Transient Electromagnetic Field Simulation," *Microwave and Optical Technology Letters,* vol. 50, no. 1, pp. 134-138, Jan. 2008.

[12] W. L. Nicomedes, R. C. Mesquita, and F. J. S. Moreira, "2-D Scattering Integral Field Equation Solution through an IMLS Meshless-Based Approach," *IEEE Trans. Magn.*, vol. 46, no. 8, pp. 2783–2486, 2010.

[13] D. Poljak, B. Jajac, and N. Kovac, "Transient Radiation of a Thin Wire Antenna Buried in a Dielectric Half Space," *Int. Ser. Adv. Boundary Elem.*., vol. 13, pp. 449–456, 2002.

[14] E. J. Kansa, "Multiqudrics - A Scattered Data Approximation Scheme with Applications to Computational Fluid-Dynamics - I Surface Approximations and Partial Derivatives," *Computer Math. Appli.,* vol. 19, pp. 127-145, 1990.

[15] W. C. Gibson, *The method of moments in electromagnetics*, New York: Chapman & Hall/CRC, Chapter 4, 2008.

[16] Z. M. Wu, "Compactly Supported Positive Definite Radial Functions," *Adv. Comput. Math.,* vol. 4, pp. 283-292, 1995.